Environmental Pollution 289 (2021) 117963

Contents lists available at ScienceDirect

Environmental Pollution

journal homepage: www.elsevier.com/locate/envpol

Radon transport events associated with the impact of a NORM repository in the SW of Europe☆

I. Gutiérrez-Álvarez [a,b,*], J.L. Guerrero [a,b], J.E. Martín [a,b], J.A. Adame [c], A. Vargas [d], J. P. Bolívar [a,b]

[a] Integrated Sciencies Department, University of Huelva, Spain
[b] Research Centre of Natural Resources, Health and the Environment (RENSMA), University of Huelva, Huelva, Spain
[c] Atmospheric Sounding Station – El Arenosillo, Atmospheric Research and Instrumentation Branch. National Institute for Aerospace Technology, INTA, Mazagón, Huelva, Spain
[d] Institute of Energy Technologies, Technical University of Catalonia, Spain

ARTICLE INFO

Keywords:
Atmospheric radon
NORM
Phosphogypsum
WRF
FLEXPART

ABSTRACT

Two radon measurement stations located to the north and south of a NORM (Naturally Occurring Radioactive Materials) repository of phosphogypsum (southwest of Europe) were used to monitor radon behavior during 2018. The stations are located at opposing sides of the repository, one in Huelva City to the north and other one in a rural area to the south. This setup aimed to identify the influence of the NORM repository on each station and use radon levels as a marker of atmospheric transport in the local area. To achieve this, a comparison was carried out with other coastal stations in the south of Spain, finding higher average concentrations in Huelva City, ~3.3 Bq m^{-3}. Hierarchical clustering was applied to identify days with different radon patterns at each Huelva station, detecting possible local radon transport events from the repository. Three events were investigated with WRF (Weather Research and Forecasting) and FLEXPART-WRF (FLEXible PARTicle dispersion model). It was found that both sampling sites required atmospheric stagnant conditions to reach high radon concentration. However, under these conditions the urban station showed high radon regardless of wind direction while the rural station also required radon transport from the repository, either directly or indirectly.

1. Introduction

Radon gas has been a useful tool in atmospheric sciences for the past few decades (Arnold et al., 2010; Botha et al., 2018; Crawford et al., 2013; Vargas et al., 2015; Zahorowski et al., 2004). It is a radioactive noble gas that is not susceptible to wet or dry atmospheric removal processes and with a half-life of 3.8 days, similar to the residence time of some air pollutants (Podstawczyńska, 2016). Its half-life is short enough not to accumulate in the atmosphere, and adequate to be a conservative tracer over several days. Natural radon has relatively constant sources inland, mainly soils rich in uranium or radium, thus generating a convenient gradient between continental and oceanic sources (Botha et al., 2018; Chambers et al., 2016; Schery and Huang, 2004), as well as differences between the planetary boundary layer and the lower troposphere (Chambers et al., 2015; Moore et al., 1973). It has been widely used as an atmospheric tracer on both regional and global scale (Arnold et al., 2010; Burton and Stewart, 1960; Grossi et al., 2018; Wilkening, 1952).

The United Nations Scientific Committee on the Effects of Atomic Radiation (UNSCEAR) reported that the dose due to inhalation of radon gas and the alpha-decay of its daughters represent more than 42% of the dose from all sources of radiation to the public (UNSCEAR, 2008). Thus, its effects on public health have been studied extensively in recent years (Darby et al., 2005; Seo et al., 2019). Concretely, radon generation and its local transport, especially near a populated area, constitutes a complex but important case of study with an increasing relevance in the literature (Akber et al., 1992; Doering, 2019; Doering et al., 2018; Podstawczyńska, 2016).

NORM (Naturally Occurring Radioactive Materials) repositories with a significant uranium or radium content can be a potential local radon source, hence becoming an interesting object of research related to radon. In the city of Huelva (southwest of Europe), there was a fertilizer

☆ This paper has been recommended for acceptance by Dr Hefa Cheng.

* Corresponding author. Integrated Sciencies Department, University of Huelva, Spain.
E-mail address: isidoro.gutierrez@dfa.uhu.es (I. Gutiérrez-Álvarez).

https://doi.org/10.1016/j.envpol.2021.117963
Received 13 April 2021; Received in revised form 19 July 2021; Accepted 11 August 2021
Available online 13 August 2021

industry complex that generated phosphoric acid for more than 40 years (1967–2010). The industrial process involved employed phosphate rock, which contained high levels of radioactive elements from the 238U series, to produce the phosphoric acid, generating phosphogypsum (PG) as a byproduct. This material, with 226Ra concentrations around 650 ± 50 Bq kg^{-1} (López-Coto et al., 2014), almost 20 times higher than 226Ra content in agricultural soils samples in the area (Abril et al., 2009), was stacked in piles near Huelva covering an area of about 100 ha in the estuary of the Tinto River, located less than 1 km from the city itself.

Previous studies proved that the repository is a potential source of radon gas (Bolívar et al., 1996; Dueñas et al., 2007). Regarding its effects on radon levels in the area, Hernández-Ceballos et al. (2015), found that radon concentrations were higher in a measurement station near Huelva when compared to a background station located 25 km to the SE, especially during 'pure-breeze' episodes. However, other effects like land-fetch or radon accumulation due to stagnant atmospheric conditions could still play a relevant role (Gutiérrez-Álvarez et al., 2019).

The main objectives of this work were: a) to detect the local influence of the Huelva PG repository on atmospheric radon, and b) use radon concentration to identify and study local transport processes. To achieve these objectives the following approach was used. First, atmospheric radon concentration data were acquired during 2018 with two measurement stations located at opposing sides of the repository, one in Huelva City to the north and other one in a rural area to the south. This data was compared with corresponding measurements at two other coastal stations located in the south of Spain to identify differences in radon behavior related to the presence of the NORM repository. After that, hierarchical clustering was employed to identify significant radon transport events that were then studied with two atmospheric modelling tools with high spatial resolution.

2. Experimental methods

2.1. Area of study

The area of study is located in the southwest of the Iberian Peninsula, centered around the city of Huelva (Spain) (Fig. 1a). This town lies near the coastline of the Atlantic Ocean, on the confluence of the Tinto and Odiel rivers, being also influenced by the Guadalquivir river valley. The wind regime in this area is characterized by the influence of SW synoptic winds coming from the Atlantic Ocean, and mesoscale transport from NE due to the neighboring Guadalquivir valley, which channels winds coming from inland (Adame et al., 2010b). In general, there is a transition from winter season, that shows more presence of NE (39%) winds, to summer, with more prevalence of winds blowing from SW (38%). Autumn and spring show intermediate results. Periods of NW winds are also experienced throughout the year, contributing 24–27% of the total, depending on the season (Adame et al., 2010a; Hernández-Ceballos, 2012).

Due to the city's proximity to the coastline, it is influenced by sea-land breezes processes when the weather conditions are favorable for its development. Two breeze patterns were observed, denominated pure and non-pure breezes (Adame et al., 2010b). Firstly, pure breezes have a first stage in the afternoon, between 12:00 and 17:00 UTC, characterized by SW winds with speeds between 1.8 and 3.2 m s^{-1}; rotating clockwise to NE winds with an average of 2.1 m s^{-1} during the night, between 03:00 to 08:00 UTC. Secondly, non-pure breeze presents identical features in the afternoon, with slower speeds, but its rotation is counter-clockwise in a NW direction during the night, after 00:00 UTC.

The NORM repository lays to the SE of the city area, as seen in Fig. 1b, and is divided in four different zones. Zones 1 and 4 were rehabilitated in 1992 and 1998, respectively, and have a layer of material on top that inhibits radon transport to the atmosphere. On the other hand, Zones 2 and 3 are still uncovered and open to the atmosphere. Zone 3 covers an area of 180 ha of PG that is predominantly flat and at ground level, as are zones 1 and 4. Zone 2 covers an area of 270 ha, but it is not at ground level, reaching an elevation of as much as 25 m above ground level for most of the area.

2.2. Measurement instrumentation

This study employed two measurement stations situated around the phosphogypsum repository located in the city of Huelva (Fig. 1b). The first measurement station was installed on a flat roof 10 m agl (above ground level) and 25 m asl (above sea level), 1.5 km to the north of the repository, in El Carmen University Campus which is part of to the University of Huelva, in a suburban area. The second was installed in a building (5 m agl) in La Rabida university campus, which is located 5 km to the south of the phosphogypsum repository, at a rural location above a small hill (23 m asl) on the other side of the Tinto River. Hourly ^{222}Rn measurements were simultaneously registered at both stations during 2018. Meteorological information was collected in the observatory managed by AEMET (Spanish Agency of Meteorology), located at a distance of 1.5 km to the northeast of the El Carmen campus (Fig. 1b). The meteorological station measured at 10 m agl and provided data (Temperature, relative humidity, pressure, wind speed and wind direction) every 10 min, which were hourly-averaged.

The radon measurement system employed in El Carmen and La

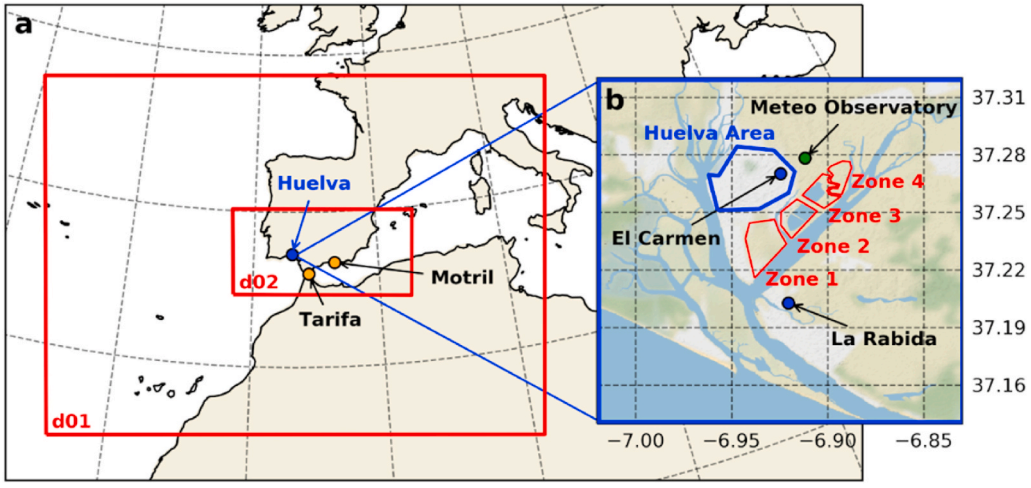

Fig. 1. Location of Huelva city in Europe, coastal measurement stations of Tarifa and Motril, and WRF simulation domains (d01 and d02) (a). Huelva measurement stations of El Carmen and La Rabida and NORM repository zones (Zones 1, 2, 3 and 4) (b).

Rabida was based on the Atmospheric Radon Monitor (ARMON), designed by INTE-UPC (Institut de Tècniques Energètiques - Universitat Politècnica de Catalunya) (Grossi et al., 2020, 2012; Vargas et al., 2015; Vargas and Ortega, 2006). This system uses a semiconductor detector inside a spherical detection volume of 20 L to detect α-particles generated by ^{218}Po ions decay. To collect these ions produced by radon decay, the moisture level is kept under 2000 ppmV and a potential difference of 8 kV is created between the inner layer of the sphere, covered with silver, and a PIPS (Passivated Implanted Planar Silicon) detector, electrically grounded and located at the top of the sphere. At the entrance of the sphere, a 1 μm filter traps all ^{222}Rn progeny generated before entering the sphere, ensuring that measured ^{218}Po ions are due to radon decay within the sphere. Both ARMON detectors were calibrated at the INTE-UPC ^{222}Rn chamber (Vargas et al., 2004). The minimum detection concentration was found to be 200 mBq m^{-3}. A detailed description of the ARMON device and its calibration can be found in Grossi et al. (2012) and Vargas et al. (2015).

As commented before, 2018 radon data from two other coastal stations were employed (Fig. 1a). These stations belong to the REA (Automatic Stations for Environmental Radiological Surveillance) network from CSN (Spanish Nuclear Safety Council). This network is composed of 25 identical measurement stations that routinely perform hourly measurements of ambient equivalent dose rate and radioactive aerosols, measuring alpha and beta radiation, radon and radioiodine concentrations to evaluate the environmental radioactivity in the Spanish territory (CSN, 2009). The aerosol monitor LB BAI 9850 from Berthold installed in these REA stations provides continuous measurements of radon progeny concentration and is described in Hernández-Ceballos et al. (2015). Data from the REA stations located in Motril and Tarifa were employed, as they represent coastal areas along the south coast of Spain, with conditions similar to those of Huelva.

2.3. Methodology and atmospheric modeling

Daily features of radon concentration at both stations were studied using hierarchical clustering of daily cycles. Instead of using natural days (midnight to midnight), the shape of the radon daily cycle was considered to perform the analysis. This was done so as to not disrupt the characteristic nocturnal radon build-up curve in the area, i.e. radon increases in the evening, growing through the night, and decreases after sunrise. For this reason, "radon days" were considered to start at 17:00 UTC, and continues for the next 24 h, thus avoiding splitting the radon evolution into two separate days.

Hierarchical clustering was applied using Python programming language and the scipySciPy package (Virtanen et al., 2020). The employed algorithm computes the Ward distance to select which clusters to join, based on minimizing the variance within clusters instead of the distance between them, forming groups with similar characteristics among members. At each iteration, the software computes the Ward distance between all clusters, finding the clusters s and t that minimize the Ward distance upon joining them in a new cluster, u, with any other remaining cluster, denoted as v. Ward distance is computed using the relation:

$$d(u,v) = \sqrt{\frac{|v|+|s|}{T}d(v,s)^2 + \frac{|v|+|t|}{T}d(v,t)^2 + \frac{|v|}{T}d(s,t)^2}$$

where $T = |v| + |s| + |t|$. When the optimal clusters s and t have been found, they are removed from the group and the newly formed cluster u is added, reducing the total number of clusters by one at each iteration. This process continues until only one cluster remains and the distances between groups on each iteration is saved. More in depth explanations about clustering techniques can be found in Bar-Joseph et al. (2001); Müllner (2011); Murtagh and Legendre (2011); and on SciPy documentation (Virtanen et al., 2020). A similar approach was applied at a single measurement station on a previous work (Gutiérrez-Álvarez et al., 2019) obtaining results that helped to understand radon behavior in the area.

To explore radon transport, meteorological fields from the ERA5 (ECMWF Reanalysis 5th Generation) global reanalysis model were used (Hersbach et al., 2020). ERA5 provides meteorological data on a 0.25-degree spatial resolution grid and 37 pressure levels. This dataset was used as input for the mesoscale numerical model Weather Research and Forecasting (WRF) designed to assist atmospheric research and forecasting applications. WRF is maintained by the Mesoscale and Microscale Meteorology Laboratory (MMM) belonging to the National Center for Atmospheric research (NCAR) of the USA (Skamarock et al., 2008). WRF simulations were configured with two large domains, d01 and d02, the first one with a 9 km resolution and the second with a 3 km resolution (Fig. 1). The resolutions were defined to follow a ratio of 1:3 between them and the ERA5 mother data resolution, as suggested by the literature (Dudhia and Wang, 2014). The simulation parameters (Table SM4) were chosen following the guidelines published in sensitivity studies in the area (Arasa et al., 2016).

The meteorological fields generated by WRF d02 domain were used as input for the FLEXPART-WRF dispersion model to study local radon transport in the city of Huelva with a high level of detail. FLEXPART (FLEXible PARTicle) is an open source Lagrangian transport and dispersion model used to simulate air parcel trajectories (Pisso et al., 2019; Stohl et al., 1998). FLEXPART-WRF is a branch of FLEXPART developed to be used with WRF output as its own input, effectively increasing the resolution of the simulations. It can be configured to run in forwards and backwards mode, hence being a useful tool to study air masses transport (Brioude et al., 2013). In our case, forward simulations were used to simulate transport from the phosphogypsum piles uncovered areas: Zone 2 and Zone 3. Due to the complexity of the PG piles, radon emissions are not fully determined as of today. Mass emitted from the repository was parametrized as a unitary value so predicted concentrations could be easily related to variable radon emissions in the future. This information was coupled with radon measurements from El Carmen and La Rabida stations to identify possible local transport processes.

3. Results and discussion

3.1. Radon overview and comparison with other coastal stations

A general characterization of radon statistics in El Carmen, La Rabida, Motril and Tarifa stations during 2018 is shown in Table SM1. In general, there is good data coverage in all stations for 2018, more than 80% in all cases, except for spring in La Rabida, which still has two thirds coverage.

The Huelva stations (El Carmen and La Rabida) appear to have a clear seasonality: the 50th percentile (median) concentrations indicate that half of the measurements in spring are below 2.0 Bq m-3, while in winter is almost five times higher, showing that spring has a much higher prevalence of lower radon concentrations than winter. Maximum radon in most seasons is above 35 Bq m^{-3}, while in spring is much lower, 23 and 17.3 Bq m^{-3} for El Carmen and La Rabida, respectively. Summer and autumn show an intermediate behavior in both stations.

Regarding Motril and Tarifa stations, the values for the 25th, 50th and 75th percentiles remain stable throughout the year, ranging from 1.07 to 1.84 Bq m^{-3} (25th), 1.97–2.67 Bq m^{-3} (50th), 3.15–4.45 Bq m^{-3} (75th). In Huelva, these ranges are only seen in spring, while the rest of the seasons systematically present higher values, confirming the lack of seasonality for Motril and Tarifa. This suggests that spring could be considered a background season for radon in Huelva stations, showing similar values to other coastal stations in the south of Spain.

This seasonality also appears in the probability density functions of hourly radon concentrations depicted in Fig. SM1. All stations show a curve that peaks somewhere between 0 and 5 Bq m^{-3} and then stretches into a long tail towards higher values. However, Motril and Tarifa show

peaks centered around 2 Bq m^{-3} for all seasons while El Carmen and La Rabida shows significant seasonal variations. In the Huelva stations, spring has more prevalence for lower values, especially in El Carmen. Summer and autumn show an intermediate behavior as their peaks are located higher than springs. Winter still shows a stretched tail but its peak is less clear than those in other seasons, as this season shows a higher probability for radon values above 5 Bq m^{-3} than any of the others. The cumulative probability density function perfectly shows these differences. Every season in Motril and Tarifa have 80% of its radon measurements under 5 Bq m^{-3}, while El Carmen and La Rabida show a transition from spring, that appears as the curve most similar to Motril and Tarifa (more than 80 % under 5 Bq m^{-3}), to winter, where only 40% of values are under the 5 Bq m^{-3} threshold.

This analysis shows significant differences between the REA coastal stations, Motril and Tarifa, and Huelva stations, El Carmen and La Rabida. To emphasize and quantify this contrast in radon characteristics, the arithmetic difference between the average hourly radon concentrations for Huelva stations and for REA coastal stations can be computed. In 2018, annual radon means are 3.3 Bq m^{-3} higher in the Huelva stations than in their coastal counterparts. These differences are more extreme in winter, where radon can be 6–7 Bq m^{-3} higher. However, spring shows similar values to the coastal stations, especially for La Rabida, as the absolute differences are close to zero. Autumn and summer show intermediate values, 4–5 and 1–2 Bq m^3 higher, respectively. Autumn is closer to winter and summer is more similar to spring. It is clear that both El Carmen and La Rabida show average radon concentrations similar to inland stations (Sesana et al., 2003; Tchorz-Trzeciakiewicz and Solecki, 2018; Vecchi et al., 2019) instead of the expected behavior of coastal stations like Motril, Tarifa and others (Crawford et al., 2013; Kobayashi et al., 2015). These differences may not be exclusively related to local meteorology, as it is expected to be similar in all studied stations, but to specific radon sources influencing Huelva radon concentrations.

3.2. Cluster characterization

As mentioned in Section 2.3, to identify and contract diurnal radon patterns in El Carmen and La Rabida stations, groups of whole (24-hr) "radon days" at both sampling sites were classified using hierarchical clustering. Days with incomplete hourly data on any of the Huelva stations were removed. The remaining set of days, 243, were used to perform the cluster characterization. Fig. 2 (a and b), displays the dendrograms obtained after clustering was applied. Dendrograms show how each cluster is related to others by drawing a U-shaped link between a cluster and its children. The top of the U-link designates a cluster merge. The two legs of the U-link direct to which clusters were merged. The length of the two legs of the U-link represents the Ward distance between the child clusters.

After analyzing the dendrograms shown in Fig. 2 (a and b), 4 clusters were selected as the optimal number of clusters in both stations: El Carmen shows several groups closer to the 100 distance value, while La Rabida also has two groups near the 100 threshold. In both cases, a distance of 115 presented enough separation from other groups to be considered as an optimal boundary, establishing 4 as the ideal number of clusters. The result of the clustering is shown in Fig. 2 (c and d). In general, both stations show clusters with similar behavior and proportion of days.

Both the stations' Cluster 1 and 3 represent days with an asymmetric peak centered around 06:00–07:00 UTC, with El Carmen station reaching higher radon concentrations. The left side of the curve (growth side) is less steep than the right side (purge side), suggesting that the radon purging process is faster than the buildup development. In both clusters, a minimum below 5 Bq m^{-3} occurs in the late afternoon. These clusters are related to wind speed under 2 m s^{-1} and ABL (Atmospheric

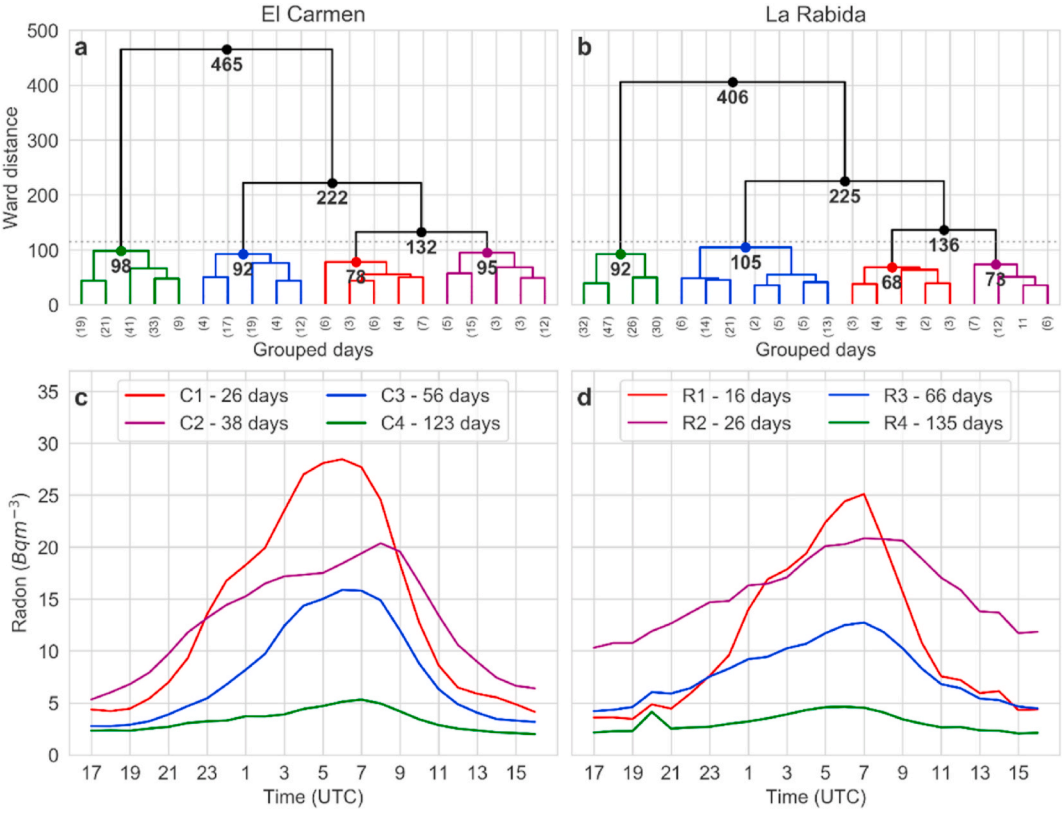

Fig. 2. Radon dendrograms for El Carmen (a) and La Rabida (b) and clusters for el Carmen (c) and La Rabida (d). The grouped days in parenthesis refer to the number of days in each subgroup. When the group has no parenthesis, it is the number of a single day not grouped yet. Numbers under group connections refer to the Ward distance between groups. The horizontal dotted line represent the war distance threshold used to define the number of groups.

Boundary Layer) height under 200 m during the night, atmospheric stability conditions that enhance surface radon accumulation. After sunrise, both wind speed and ABL height increase significantly, facilitating the radon purging process (Fig. SM2 and Fig. SM3). These results were similar to those obtained in a previous study (Gutiérrez-Álvarez et al., 2019).

At both stations Cluster 4 is the most populated cluster, showing a flat radon behavior throughout the whole day. Fig. SM2 and Fig. SM3 show that this cluster is characterized by systematically higher wind speeds and ABL height than the rest of the clusters. This is especially relevant throughout the night, when wind speed and ABL height stay above 2 m s^{-1} and 400 m, respectively.

Cluster 2 in La Rabida is the most different among the stations, showing a clearly unique behavior. Although both stations climb to similar maximum concentrations during the night (00:00 to 09:00 UTC), La Rabida starts and ends above 10 Bq m^{-3}, while El Carmen only shows half of those concentrations at the beginning and the end of the cluster. This last behavior is also shown by Cluster 3, albeit to a lesser extent. The lack of radon dispersion in the afternoon is linked to stagnant atmospheric conditions, i.e. low ABL and wind speeds, as can be seen in Fig. SM2 and SM3. Cluster 2 is the only cluster that does not show an increase in wind speed above 3 m s^{-1} during the day. In addition, ABL height only reach a maximum altitude of 600 m, staying under 200 m during most of the day.

Clusters 1 and 2 are more populated in El Carmen than in La Rabida, i.e. there are more days with high radon in the former than in the latter. Consequently, Clusters 3 and 4 contain more days in La Rabida, meaning that La Rabida has more low radon days in general. This suggests that high radon events are more frequent in El Carmen than in La Rabida, probably due to the former being closer to the repository than the latter. El Carmen also shows a better capacity to purge radon afterwards than La Rabida, which could be related to the differences between the urban and rural environments of each station. Convection processes typical of city's heat islands could help to vertically dilute radon in El Carmen measurement station.

Although the clusters are not entirely similar in both stations, it would be interesting to study the coincidence in time of clusters associated to the same behavior on both stations. This would help to investigate how frequently high radon events occur on both stations and how frequently they do not. The cluster assignation of each station was compared to the other, checking the correspondence of each clusters on both stations. The results can be seen in Table SM3 and Fig. SM4. As expected, most days have the same cluster assignation on both stations, which means that radon behaves in a similar way in both stations. However, there is some asymmetry, since there are a significant number of days with high radon in El Carmen but low in La Rabida, i.e. C1 can be observed together with R2, R3 and R4. Conversely, the reverse situation is not as frequent, being only three cases where R1 coincides with C2 and no cases with C3 and C4. This leads to generally higher radon levels for El Carmen than La Rabida when cluster behavior on each station is compared (Fig. SM4). As both stations are close to one another, this could point out the influence of a local source that is more likely to affect El Carmen than La Rabida.

3.3. Event analysis

The differences between cluster assignation provide a criterion to identify and study radon events, as days with different clusters in El Carmen and La Rabida are more likely to provide insights about local radon transport in the area. Consequently, the results of the hierarchical clustering were used to identify three events that were studied in depth using FLEXPART-WRF transport model simulations. With the exception of the first event, which shows a base case with high radon concentrations in both sampling sites, the rest feature different radon daily curves at each station, allowing to study the conditions that caused the differences between them.

The first event, A, features a period that was classified as a high radon concentration day in both El Carmen and La Rabida stations (Clusters C1-R1). The second event, B, corresponds to a period where El Carmen presented high radon levels (Cluster C1), but La Rabida had lower radon concentrations on that same day (Clusters R3 or R4). Lastly, event C features an interesting set of days where La Rabida had a series of consecutives days with radon concentrations above 10 Bq m^{-3} during most of the day (Cluster R2), while El Carmen showed a classical radon daily curve (Clusters C2 and C3).

3.3.1. Event A: high radon clusters at both stations (C1-R1) on 11/08/2018

The first event (11/08/2018) occurs within a set of four days in August with days varying between SW and NW wind direction, covering from the 10th to the 13th of August 2018 (Fig. 3a–c). This period is characterized by mesoscale conditions, mainly non-pure breezes on the 10/08, 12/08 and 13/08. The 11/08 shows a general similarity with a pure breeze pattern but in this case there is an irregular NE-N-NW direction during the night with low wind speeds, increasing its speed and rotation to SW in the afternoon.

The first day, 10/08, shows wind speeds decreasing during radon growth period but still greater than 2 m s^{-1}, with an ABL above 200 m. Radon levels during this day are similar in both stations, remaining under 10 Bq m^{-3}. The next day, 11/08, classified as a high radon day on both stations, shows a wind regime with a general N direction, alternating between NW and NE during the radon growth, with wind speed under 2 m s^{-1}, and pointing to SW during purge. ABL heights are generally low during the night with two minima below 100 m, corresponding to two radon peaks in El Carmen station, at 21:00 and 06:00 UTC. La Rabida only shows one peak around 07:00 UTC, being similar to the peak observed in El Carmen both in time and concentration. On the 12/08, the ABL remains under 100 m during the nighttime, with wind speed lower than 2 m s^{-1}, allowing radon growth in El Carmen and La Rabida, although being less significant in the latter than in the former. On the 13/08, ABL levels are above 400 m and there is an increasing wind speed greater than 2 m s^{-1}, leading to low radon concentration.

FLEXPART-WRF was employed to simulate the local transport and study the selected events. Focusing on the second day of this event, Fig. 3d–g shows that the radon plume from the PG piles did not go over La Rabida during the first peak occurring on the 10/08 at 21:00 UTC. After that, the breeze pattern caused the wind to rotate clockwise and get closer to La Rabida direction, which was under a direct influence at 07:00 UTC, when the radon concentration reached its maximum in the southern station. It is important to note that El Carmen shows a similar evolution on the 11/08 between 03:00 and 12:00 UTC, probably due to the low wind speeds and ABL. Radon behavior during this period suggests that La Rabida requires direct transport from the PG piles, as it is located further away from the PG repository, while El Carmen could be affected by small-scale air movements such as submeso motions (Mahrt, 2014) or diffusion, possibly related to differences in land-use and the formation of an urban heat island circulation.

3.3.2. Event B: high radon cluster at El Carmen and low in La Rabida (C1-R3) on 13/10/2018

The second event (13/10/2018) occurs within a 4-day period from the 11th to the 14th of October 2018, comprising two days governed by mesoscale process between days with synoptic winds. The two central days show a pure-breeze wind regime, low speed wind from NE during the night and higher wind speed from SW during the afternoon, bracketed by two days with strong winds from SW and NW direction, respectively (Fig. 4a–c).

On the first and last day, the 11/10 and 14/10, radon appears flat under 5 Bq m^{-3}, as expected due to the high wind speeds and ABL height. The following day, the 12/10, a pure-breeze pattern appears, the ABL height drops under 100 m at night and wind speed under 2 m s^{-1} after 00:00 UTC. This causes a small growth in radon levels in El Carmen

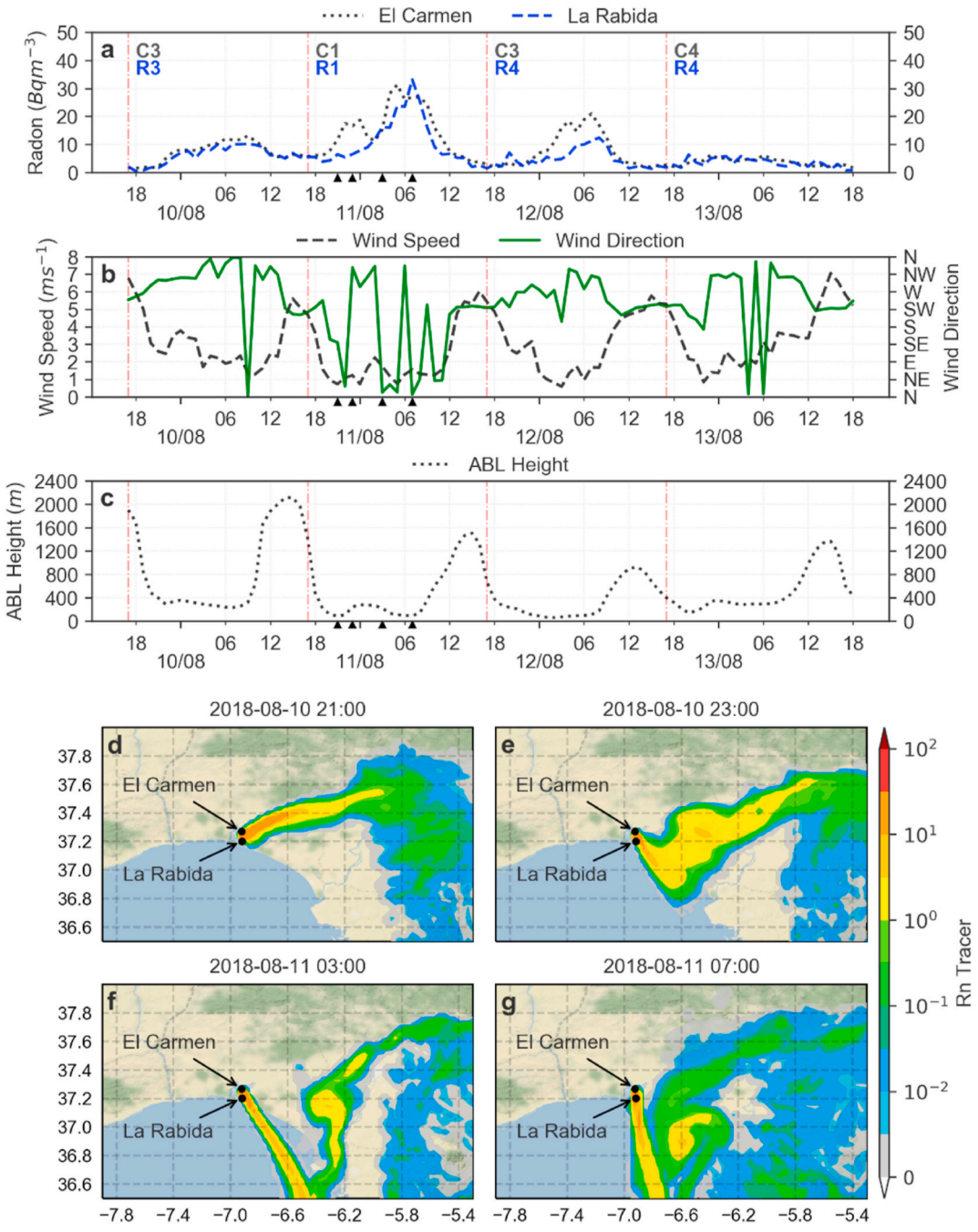

Fig. 3. Event A radon concentrations evolution in El Carmen and La Rabida (a), wind speed and direction temporal evolution (b), ABL hourly variation obtained from ERA5 (ECMWF) (c) from August 10th to 13th, 2018. Radon spatial distribution simulated by FLEXPART-WRF for August 10th at 21:00 UTC (d), August 10th at 23:00 UTC (e), August 11th at 03:00 UTC (f), and August 11th at 07:00 UTC (g).

station, although not surpassing 10 Bq m^{-3}. La Rabida station shows two small peaks around 03:00 and 07:00 UTC, with 5 and 10 Bq m^{-3}, respectively. This breeze pattern repeats almost identically on the next day, the 13/10, but on this occasion wind speed and ABL height drop at 18:00 UTC (12/10). Wind speed stay under 2 m s^{-1} throughout the growth period and ABL height stay under 100 m for the next 12 h. This causes a significant increase in radon levels in El Carmen, which grows up to 30 Bq m^{-3} at 07:00 UTC, decreasing afterwards. La Rabida station shows a humble increase at the same time as El Carmen, but stay constant until 02:00 UTC, when a sudden increase creates a radon peak of 20 Bq m^{-3}, decreasing as quickly as it appeared to 10 Bq m^{-3}, and fading definitively at sunrise (8:00 UTC).

This series of days appears interesting, showing a radon-free ambient atmosphere that develops into a period of radon growth that affects each station differently. Considering the behavior in El Carmen and La Rabida, and its proximity between each other, the influence of long-range radon transport by an external source seems unlikely, as it would have affected both stations equally. FLEXPART-WRF simulations provides an explanation for radon in La Rabida station on the central days of this event caused by a breeze-pattern. On the third day, the first part of the breeze consists of SW winds pushing the radon plume to the NE (Fig. 4d). During the next hours, the wind direction starts to rotate clockwise until it reaches the NW direction, around 20:00–22:00 UTC (Fig. 4e), pushing radon towards La Rabida station and causing a radon rising during the late evening, at 21:00 UTC. Afterwards, the breeze pattern has completely reversed its direction (Fig. 4f) and the air mass that initially

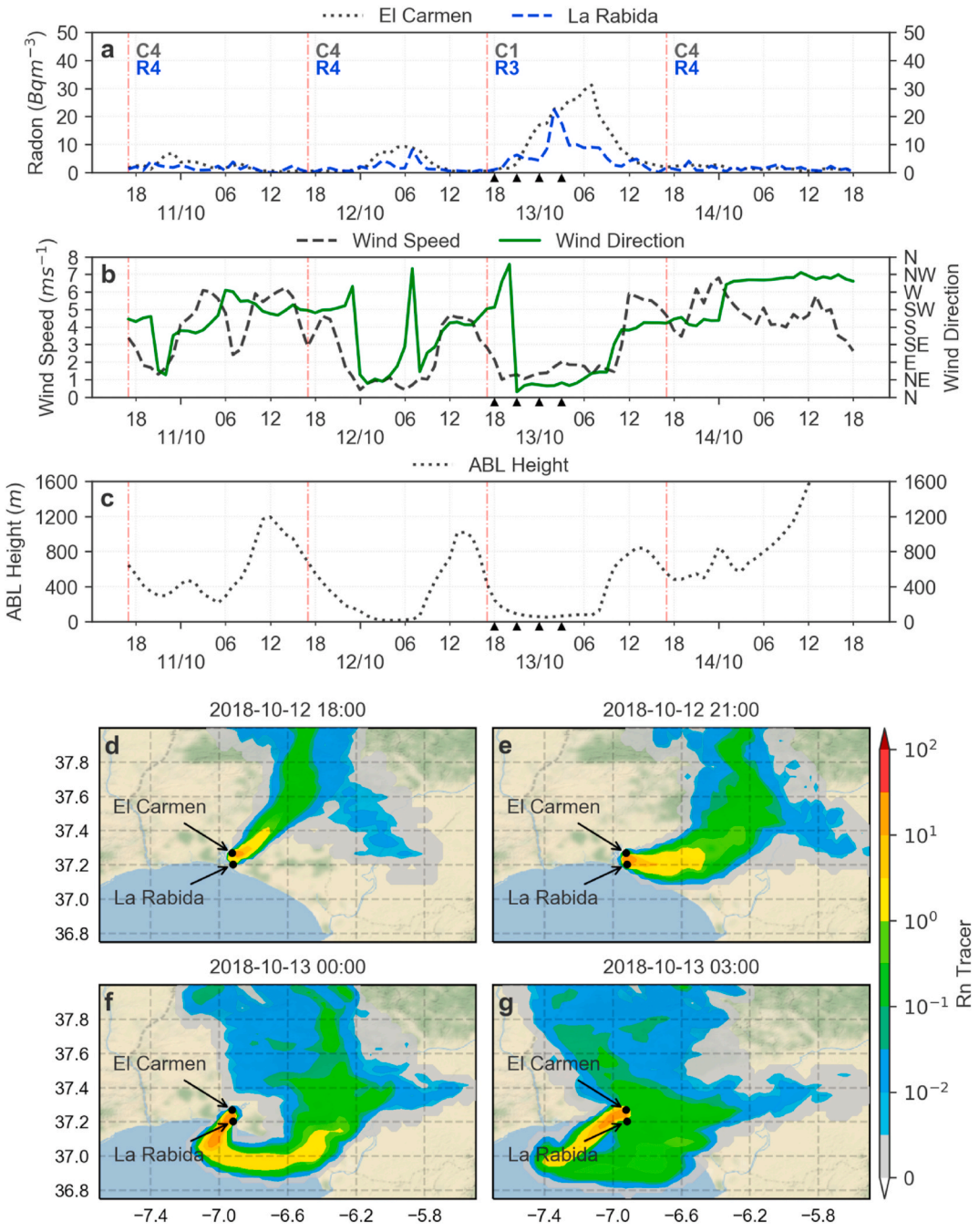

Fig. 4. Event B radon concentrations evolution in El Carmen and La Rabida (a), wind speed and direction temporal evolution (b), ABL hourly variation obtained from ERA5 (ECMWF) (c) from October 11th to 14th, 2018. Radon spatial distribution simulated by FLEXPART-WRF for October 12th at 18:00 UTC (d), October 12th at 21:00 UTC (e), October 13th at 00:00 UTC (f), and October 13th at 03:00 UTC (g).

travelled inland starts to go back towards both stations, hitting them around 03:00 UTC on the 13/10 (Fig. 4g). This radon comeback causes a second peak in La Rabida, separated 5 h from the first, building up with the radon already accumulated in the area due to the low ABL height. After this second wave of radon goes away, and radon-free air reaches the area of study, radon levels decrease, helped by the rising ABL height during the daytime.

3.3.3. Event C: constant high radon concentration at La Rabida (C3-R2, C2-R2) on 14–17/01/2018

The final study period shows a set of four days during winter, from the 14th to the 17th of January 2018 (Fig. 5a–c), which belongs to R2 cluster, featuring radon levels above 10 Bq m^{-3} in La Rabida during the whole day. It comprises a set of days under the influence of synoptic winds from NW-N-NE with low wind speeds and low nocturnal ABL height.

In this case, different radon patterns can be seen on each measurement station. La Rabida displays an irregular radon pattern of high radon concentrations, varying between 10 and 20 Bq m^{-3}, while El Carmen presents the expected daily cycle increasing during the nighttime and decreasing when the sun rises, rarely exceeding the 20 Bq m^{-3} threshold. High ABL levels and high wind speeds were connected to lower radon concentration in El Carmen during afternoons, whilst low ABL heights and low winds resulted in modest radon peaks at night. Nocturnal wind speeds remain around 1.5 m s^{-1} the majority of the time, only surpassing the 2 m s^{-1} on 14/01 between 10:00 and 18:00

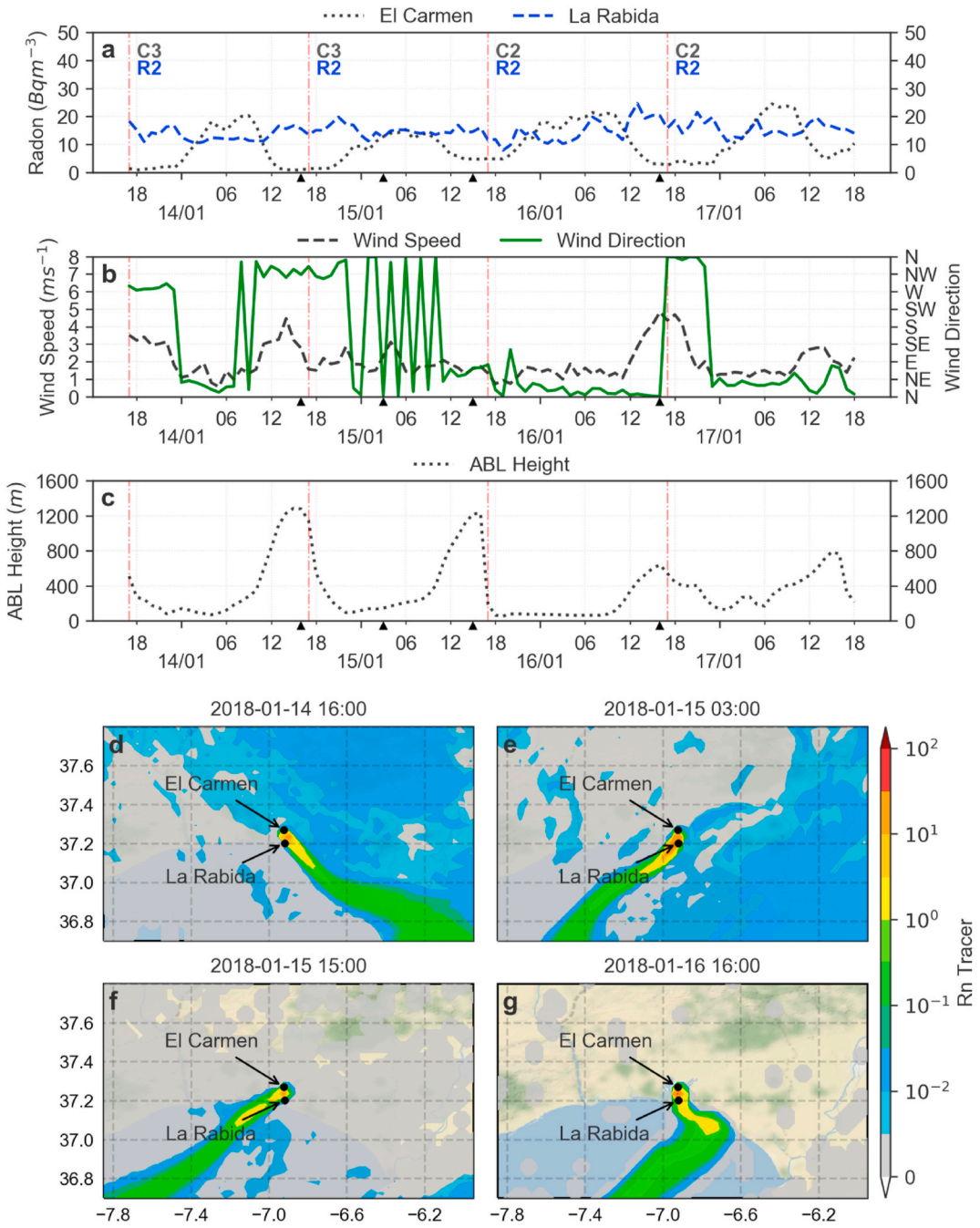

Fig. 5. Event C radon concentrations evolution in El Carmen and La Rabida (a), wind speed and direction temporal evolution (b), ABL hourly variation obtained from ERA5 (ECMWF) (c) from January 14th to 17th, 2018. Radon spatial distribution simulated by FLEXPART-WRF for January 14th at 16:00 UTC (d), January 15th at 03:00 UTC (e), January 15th at 15:00 UTC (f), and January 16th at 16:00 UTC (g).

UTC and 16/01 between 12:00 and 21:00 UTC. The ABL height on the first two days has a first stage under 200 m between 21:00 and 06:00 UTC, significantly rising between 06:00 UTC and 13:00 UTC. Afterwards, on the 15/01, ABL height settles under 100 m between 18:00 UTC and 08:00 UTC on the 16/01, rising again and staying above 200 m during the rest of the event.

On the 14/01, the wind shifted from an initial W direction and started to hover around the NW-NE sector for the next three days. These constant but slow winds possibly transported radon from the PG piles to La Rabida station constantly, as can be seen in Fig. 5d–g. On the 14/10 at 16:00 UTC, wind came initially from the NW (Fig. 5d) but then slowly rotates clockwise until reaching NE direction 11 h later (Fig. 5e). This wind direction was relatively stable from 15:00 UTC on the 15/10 to 12:00 UTC on the 16/10, when the wind direction shifted again to NW, but rotating counterclockwise on this occasion (Fig. 5f–g). The general wind regime, blowing from the NW-NE, as it is frequent in winter, was transporting radon from the repository to the south, broadly in the direction of La Rabida. This air movement, coupled with slow wind speeds, may have helped radon to disperse and also allowed to diffuse enough from the main transport plume, reaching constantly La Rabida measurement station while these conditions held.

4. Conclusions

The influence of a NORM (Normally Occurring Radioactive Materials) repository on the radon concentration in its nearby area was

detected using observations from two stations in opposite sides of the repository, El Carmen, inside an urban environment, and La Rabida, within a rural area. The lagrangian dispersion model FLEXPART-WRF in combination with the mesoscale simulation model WRF were used to investigate radon transport processes. Radon measurements for El Carmen and La Rabida were classified using hierarchical clustering. This clustering classification was used to identify group of days with different radon behavior at each station, allowing to recognize useful events to study local transport. Radon transport simulations from the NORM repository were then carried out with FLEXPART-WRF, elucidating the air mass movement and explaining the radon evolution in relation to a local source.

The measured radon concentrations at the two main sites were compared with two coastal stations from the REA network managed by CSN. Compared to those, El Carmen and La Rabida show average radon concentrations 3.5 and 3.2 Bq m^{-3} higher, respectively. These differences are higher in winter, 6.2 and 7.2 Bq m^{-3}, and lower in spring, 0.03 and 0.17 Bq m^{-3}. The presence of the local repository as a local radon source produces seasonal and daily patterns that increase the background radon levels.

Clustering classification suggested generally similar daily radon patterns on both stations, where radon built up during the nighttime under low wind speed and low ABL height conditions, being removed during the daytime by mixing into the deeper ABL. Nevertheless, the classification reflected a better daytime purging efficiency in the urban station than in the rural one. There was a higher occurrence of clusters related to high radon concentration days in El Carmen than in La Rabida. Considering the former is located closer to the repository than the latter but still close to each other. This fact suggests that any difference between them, in relation to radon concentrations, is mainly caused by local processes. Therefore, the overall influence of regional medium-long range source might have is not as significant as the contribution due to the PG piles.

Simulations with FLEXPART-WRF suggested that radon concentrations in El Carmen do not require direct transport but only stagnant atmospheric conditions, i.e. low wind speeds and ABL height. However, for the three studied events, La Rabida only had high radon cluster assignations when there was direct transport from the NORM repository in addition to the stagnant atmospheric conditions. This could be explained considering the geography of the area, since air masses have to travel further from the repository to reach La Rabida. On the other hand, El Carmen could be affected by small-scale air movements, such as submeso motions or diffusion, that raised the possibility of radon circulation towards the city due to the formation of an urban heat island.

Declaration of competing interest

The authors declare that they have no known competing financial interests or personal relationships that could have appeared to influence the work reported in this paper.

Acknowledgements

This research was supported by the Spanish Ministry of Science, Innovation and Universities, by the project 'Fluxes of radionuclides emitted by the PG piles located at Huelva; assessment of the dispersion, radiological risks and remediation proposals' (Ref.: CTM2015-68628-R). It is important to reiterate the significant contribution of CSN to this research providing radon measurements from the REA network. Special thanks are given to Antonio Padilla for his invaluable technical support and know-how. Resources supporting this work were provided by the CEAFMC and Universidad de Huelva High Performance Computer (HPC@UHU) funded by ERDF/MINECO project UNHU-15CE-2848.

Appendix A. Supplementary data

Supplementary data to this article can be found online at https://doi.org/10.1016/j.envpol.2021.117963.

Credit author statement

I. Gutiérrez-Álvarez: Conceptualization, Software, Formal analysis, Investigation, Data curation, Writing – original draft, Writing – review & editing, Visualization **J.L. Guerrero**: Formal analysis, Investigation, Writing – review & editing, Visualization **J.E. Martín**: Conceptualization Software, Investigation, Data curation, Writing – review & editing, Visualization **J.A. Adame**: Conceptualization, Validation, Writing – review & editing **A. Vargas**: Validation, Writing – review & editing **J.P. Bolívar**: Conceptualization, Writing – review & editing Supervision, Project administration, Funding acquisition

References

Abril, J.M., García-Tenorio, R., Manjón, G., 2009. Extensive radioactive characterization of a phosphogypsum stack in SW Spain: 226Ra, 238U, 210Po concentrations and 222Rn exhalation rate. J. Hazard Mater. 164, 790–797. https://doi.org/10.1016/J.JHAZMAT.2008.08.078.

Adame, J.A., Bolívar, J.P., de la Morena, B., Lammel, A., Gerhard, J., 2010a. Surface ozone measurements in the southwest of the iberian Peninsula (Huelva, Spain). Environ. Sci. Pollut. Res. 17, 355–368. https://doi.org/10.1007/s11356-008-0098-9.

Adame, J.A., Serrano, E., Bolívar, J.P., de la Morena, B.A., Adame, J.A., Serrano, E., Bolívar, J.P., Morena, B.A. de la, 2010b. On the tropospheric ozone variations in a coastal area of southwestern Europe under a mesoscale circulation. J. Appl. Meteorol. Climatol. 49, 748–759. https://doi.org/10.1175/2009JAMC2097.1.

Akber, R.A., Johnston, A., Pfitzner, J., 1992. Public radiation exposure due to radon transport from a uranium mine. Radiat. Protect. Dosim. 45, 137–140. https://doi.org/10.1093/rpd/45.1-4.137.

Arasa, R., Porras, I., Domingo-Dalmau, A., Picanyol, M., Codina, B., González, M.Á., Piñón, J., 2016. Defining a standard methodology to obtain optimum WRF configuration for operational forecast: application over the port of Huelva (southern Spain). Atmos. Clim. Sci. 6, 329–350. https://doi.org/10.4236/acs.2016.62028.

Arnold, D., Vargas, A., Vermeulen, A.T., Verheggen, B., Seibert, P., 2010. Analysis of radon origin by backward atmospheric transport modelling. Atmos. Environ. 44, 494–502. https://doi.org/10.1016/j.atmosenv.2009.11.003.

Bar-Joseph, Z., Gifford, D.K., Jaakkola, T.S., 2001. Fast optimal leaf ordering for hierarchical clustering. Bioinformatics 17, S22–S29. https://doi.org/10.1093/bioinformatics/17.suppl_1.S22.

Bolívar, J.P., García-Tenorio, R., García-León, M., 1996. Radioactive impact of some phosphogypsum piles in soils and salt marshes evaluated by γ-ray spectrometry. Appl. Radiat. Isot. 47, 1069–1075. https://doi.org/10.1016/S0969-8043(96)00108-X.

Botha, R., Labuschagne, C., Williams, A.G., Bosman, G., Brunke, E.-G., Rossouw, A., Lindsay, R., 2018. Characterising fifteen years of continuous atmospheric radon activity observations at Cape Point (South Africa). Atmos. Environ. 176, 30–39. https://doi.org/10.1016/J.ATMOSENV.2017.12.010.

Brioude, J., Arnold, D., Stohl, A., Cassiani, M., Morton, D., Seibert, P., Angevine, W., Evan, S., Dingwell, A., Fast, J.D., Easter, R.C., Pisso, I., Burkhart, J., Wotawa, G., 2013. The Lagrangian particle dispersion model FLEXPART-WRF version 3.1. Geosci. Model Dev 6, 1889–1904. https://doi.org/10.5194/gmd-6-1889-2013.

Burton, W.M., Stewart, N.G., 1960. Use of long-lived natural radioactivity as an atmospheric tracer. Nature 186, 584–589. https://doi.org/10.1038/186584a0.

Chambers, S.D., Wang, F., Williams, A.G., Xiaodong, D., Zhang, H., Lonati, G., Crawford, J., Griffiths, A.D., Ianniello, A., Allegrini, I., 2015. Quantifying the influences of atmospheric stability on air pollution in Lanzhou, China, using a radon-based stability monitor. Atmos. Environ. 107, 233–243. https://doi.org/10.1016/J.ATMOSENV.2015.02.016.

Chambers, S.D., Williams, A.G., Conen, F., Griffiths, A.D., Reimann, S., Steinbacher, M., Krummel, P.B., Steele, L.P., Van Der Schoot, M.V., Galbally, I.E., Molloy, S.B., Barnes, J.E., 2016. Towards a universal baseline characterisation of air masses for high-and low-altitude observing stations using radon-222. Aerosol Air Qual. Res. 16, 885–899. https://doi.org/10.4209/aaqr.2015.06.0391.

Crawford, J., Zahorowski, W., Cohen, D.D., Chambers, S., Stelcer, E., Werczynski, S., 2013. Estimating the near-surface daily fine aerosol load using hourly Radon-222 observations. Atmos. Pollut. Res. 4, 1–13. https://doi.org/10.5094/APR.2013.001.

CSN, 2009. Red de estaciones automáticas de vigilancia radiológica ambiental (REA) del Consejo de Seguridad Nuclear. Colección Informes Técnicos.

Darby, S., Hill, D., Auvinen, A., Barros-Dios, J.M., Baysson, H., Bochicchio, F., Deo, H., Falk, R., Forastiere, F., Hakama, M., Heid, I., Kreienbrock, L., Kreuzer, M., Lagarde, F., Mäkeläinen, I., Muirhead, C., Oberaigner, W., Pershagen, G., Ruano-Ravina, A., Ruosteenoja, E., Schaffrath Rosario, A., Tirmarche, M., Tomášek, L., Whitley, E., Wichmann, H.E., Doll, R., 2005. Radon in homes and risk of lung cancer: collaborative analysis of individual data from 13 European case-control studies. Br. Med. J. 330, 223–226. https://doi.org/10.1136/bmj.38308.477650.63.

Doering, C., 2019. A new background subtraction method for assessing public radiation exposure due to radon transport from an uranium mine. Radiat. Protect. Dosim. 186, 530–535. https://doi.org/10.1093/rpd/ncz141.

Doering, C., McMaster, S.A., Johansen, M.P., 2018. Modelling the dispersion of radon-222 from a landform covered by low uranium grade waste rock. J. Environ. Radioact. 192, 498–504. https://doi.org/10.1016/j.jenvrad.2018.07.024.

Dudhia, J., Wang, W., 2014. WRF Advanced Usage and Best Practices, vol. 35.

Dueñas, C., Liger, E., Cañete, S., Pérez, M., Bolívar, J.P., 2007. Rn from phosphogypsum piles located at the Southwest of Spain. J. Environ. Radioact. 95, 63–74. https://doi.org/10.1016/j.jenvrad.2007.01.012.

Grossi, C., Arnold, D., Adame, J.A., López-Coto, I., Bolívar, J.P., De La Morena, B.A., Vargas, A., 2012. Atmospheric 222Rn concentration and source term at El Arenosillo 100 m meteorological tower in southwest Spain. Radiat. Meas. 47, 149–162. https://doi.org/10.1016/j.radmeas.2011.11.006.

Grossi, C., Chambers, S.D., Llido, O., Vogel, F.R., Kazan, V., Capuana, A., Werczynski, S., Curcoll, R., Delmotte, M., Vargas, A., Morguí, J.A., Levin, I., Ramonet, M., 2020. Intercomparison study of atmospheric 222Rn and 222Rn progeny monitors. Atmos. Meas. Tech. 13, 2241–2255. https://doi.org/10.5194/AMT-13-2241-2020.

Grossi, C., Vogel, F.R., Curcoll, R., Àgueda, A., Vargas, A., Rodó, X., Morguí, J.-A., 2018. Study of the daily and seasonal atmospheric CH4 mixing ratio variability in a rural Spanish region using 222Rn tracer. Atmos. Chem. Phys. 18, 5847–5860. https://doi.org/10.5194/acp-18-5847-2018.

Gutiérrez-Álvarez, I., Guerrero, J.L., Martín, J.E., Adame, J.A., Vargas, A., Bolívar, J.P., 2019. Radon behavior investigation based on cluster analysis and atmospheric modelling. Atmos. Environ. 201, 50–61. https://doi.org/10.1016/j.atmosenv.2018.12.010.

Hernández-Ceballos, M.A., 2012. Caracterización meteorológica y modelización de Andalucía Occidental. University of Huelva.

Hernández-Ceballos, M.A., Vargas, A., Arnold, D., Bolívar, J.P., 2015. The role of mesoscale meteorology in modulating the ^{222}Rn concentrations in Huelva (Spain) - impact of phosphogypsum piles. J. Environ. Radioact. 145, 1–9. https://doi.org/10.1016/j.jenvrad.2015.03.023.

Hersbach, H., Bell, B., Berrisford, P., Hirahara, S., Horányi, A., Muñoz-Sabater, J., Nicolas, J., Peubey, C., Radu, R., Schepers, D., Simmons, A., Soci, C., Abdalla, S., Abellan, X., Balsamo, G., Bechtold, P., Biavati, G., Bidlot, J., Bonavita, M., De Chiara, G., Dahlgren, P., Dee, D., Diamantakis, M., Dragani, R., Flemming, J., Forbes, R., Fuentes, M., Geer, A., Haimberger, L., Healy, S., Hogan, R.J., Hólm, E., Janisková, M., Keeley, S., Laloyaux, P., Lopez, P., Lupu, C., Radnoti, G., de Rosnay, P., Rozum, I., Vamborg, F., Villaume, S., Thépaut, J.N., 2020. The ERA5 global reanalysis. Q. J. R. Meteorol. Soc. 146, 1999–2049. https://doi.org/10.1002/qj.3803.

Kobayashi, Y., Yasuoka, Y., Omori, Y., Nagahama, H., Sanada, T., Muto, J., Suzuki, T., Homma, Y., Ihara, H., Kubota, K., Mukai, T., 2015. Annual variation in the atmospheric radon concentration in Japan. J. Environ. Radioact. 146, 110–118. https://doi.org/10.1016/J.JENVRAD.2015.04.007.

López-Coto, I., Mas, J.L., Vargas, A., Bolívar, J.P., 2014. Studying radon exhalation rates variability from phosphogypsum piles in the SW of Spain. J. Hazard Mater. 280, 464–471. https://doi.org/10.1016/j.jhazmat.2014.07.025.

Mahrt, L., 2014. Stably Stratified Atmospheric Boundary Layers, pp. 23–45. https://doi.org/10.1146/ANNUREV-FLUID-010313-141354.

Moore, H.E., Poet, S.E., Martell, E.A., 1973. 222 Rn, 210 Pb, 210 Bi, and 210 Po profiles and aerosol residence times versus altitude. J. Geophys. Res. 78, 7065–7075. https://doi.org/10.1029/JC078i030p07065.

Müllner, D., 2011. Modern Hierarchical, Agglomerative Clustering Algorithms.

Murtagh, F., Legendre, P., 2011. Ward's hierarchical clustering method: clustering criterion and agglomerative algorithm [WWW document]. J. Classif. https://doi.org/10.1007/s00357-014-9161-z.

Pisso, I., Sollum, E., Grythe, H., Kristiansen, N., Cassiani, M., Eckhardt, S., Arnold, D., Morton, D., Thompson, R.L., Groot Zwaaftink, C.D., Evangeliou, N., Sodemann, H., Haimberger, L., Henne, S., Brunner, D., Burkhart, J.F., Fouilloux, A., Brioude, J., Philipp, A., Seibert, P., Stohl, A., 2019. The Lagrangian particle dispersion model FLEXPART version 10.3. Geosci. Model Dev. Discuss. 1–67. https://doi.org/10.5194/gmd-2018-333.

Podstawczyńska, A., 2016. Differences of near-ground atmospheric Rn-222 concentration between urban and rural area with reference to microclimate diversity. Atmos. Environ. 126, 225–234. https://doi.org/10.1016/J.ATMOSENV.2015.11.037.

Schery, S.D., Huang, S., 2004. An estimate of the global distribution of radon emissions from the ocean. Geophys. Res. Lett. 31, L19104. https://doi.org/10.1029/2004GL021051.

Seo, S., Ha, W.H., Kang, J.K., Lee, D., Park, S., Kwon, T.E., Jin, Y.W., 2019. Health effects of exposure to radon: implications of the radon bed mattress incident in Korea. Epidemiol. Health 41, e2019004. https://doi.org/10.4178/epih.e2019004.

Sesana, L., Caprioli, E., Marcazzan, G.M., 2003. Long period study of outdoor radon concentration in Milan and correlation between its temporal variations and dispersion properties of atmosphere. J. Environ. Radioact. 65, 147–160. https://doi.org/10.1016/S0265-931X(02)00093-0.

Skamarock, C., Klemp, B., Dudhia, J., Gill, O., Barker, D., Duda, G., Huang, X., Wang, W., Powers, G., 2008. A Description of the Advanced Research WRF Version 3. https://doi.org/10.5065/D68S4MVH.

Stohl, A., Hittenberger, M., Wotawa, G., 1998. Validation of the Lagrangian particle dispersion model FLEXPART against large-scale tracer experiment data. Atmos. Environ. 32, 4245–4264. https://doi.org/10.1016/S1352-2310(98)00184-8.

Tchorz-Trzeciakiewicz, D.E., Solecki, A.T., 2018. Variations of radon concentration in the atmosphere. Gamma dose rate. Atmos. Environ. 174, 54–65. https://doi.org/10.1016/J.ATMOSENV.2017.11.033.

UNSCEAR, 2008. Sources, Effects and Risks of Ionizing Radiation. In: Radiation Research, vol. I. https://doi.org/10.2307/3577647.

Vargas, A., Arnold, D., Adame, J.A., Grossi, C., Hernández-Ceballos, M.A., Bolívar, J.P., 2015. Analysis of the vertical radon structure at the Spanish "El arenosillo" tower station. J. Environ. Radioact. 139, 1–17. https://doi.org/10.1016/j.jenvrad.2014.09.018.

Vargas, A., Ortega, X., 2006. Influence of environmental changes on continuous radon monitors. Results of a Spanish intercomparison exercise. Radiat. Protect. Dosim. 121, 303–309. https://doi.org/10.1093/rpd/ncl036.

Vargas, A., Ortega, X., Matarranz, J.L.M., 2004. Traceability of radon-222 activity concentration in the radon chamber at the technical university of Catalonia (Spain). Nucl. Instruments Methods Phys. Res. Sect. A Accel. Spectrometers, Detect. Assoc. Equip. 526, 501–509. https://doi.org/10.1016/j.nima.2004.02.022.

Vecchi, R., Piziali, F.A., Valli, G., Favaron, M., Bernardoni, V., 2019. Radon-based estimates of equivalent mixing layer heights: a long-term assessment. Atmos. Environ. 197, 150–158. https://doi.org/10.1016/J.ATMOSENV.2018.10.020.

Virtanen, P., Gommers, R., Oliphant, T.E., Haberland, M., Reddy, T., Cournapeau, D., Burovski, E., Peterson, P., Weckesser, W., Bright, J., van der Walt, S.J., Brett, M., Wilson, J., Millman, K.J., Mayorov, N., Nelson, A.R.J., Jones, E., Kern, R., Larson, E., Carey, C.J., Polat, İ., Feng, Y., Moore, E.W., VanderPlas, J., Laxalde, D., Perktold, J., Cimrman, R., Henriksen, I., Quintero, E.A., Harris, C.R., Archibald, A.M., Ribeiro, A.H., Pedregosa, F., van Mulbregt, P., Vijaykumar, A., Bardelli, A., Pietro Rothberg, A., Hilboll, A., Kloeckner, A., Scopatz, A., Lee, A., Rokem, A., Woods, C.N., Fulton, C., Masson, C., Häggström, C., Fitzgerald, C., Nicholson, D.A., Hagen, D.R., Pasechnik, D.V., Olivetti, E., Martin, E., Wieser, E., Silva, F., Lenders, F., Wilhelm, F., Young, G., Price, G.A., Ingold, G.L., Allen, G.E., Lee, G.R., Audren, H., Probst, I., Dietrich, J.P., Silterra, J., Webber, J.T., Slavič, J., Nothman, J., Buchner, J., Kulick, J., Schönberger, J.L., de Miranda Cardoso, J.V., Reimer, J., Harrington, J., Rodríguez, J.L.C., Nunez-Iglesias, J., Kuczynski, J., Tritz, K., Thoma, M., Newville, M., Kümmerer, M., Bolingbroke, M., Tartre, M., Pak, M., Smith, N.J., Nowaczyk, N., Shebanov, N., Pavlyk, O., Brodtkorb, P.A., Lee, P., McGibbon, R.T., Feldbauer, R., Lewis, S., Tygier, S., Sievert, S., Vigna, S., Peterson, S., More, S., Pudlik, T., Oshima, T., Pingel, T.J., Robitaille, T.P., Spura, T., Jones, T.R., Cera, T., Leslie, T., Zito, T., Krauss, T., Upadhyay, U., Halchenko, Y.O., Vázquez-Baeza, Y., 2020. SciPy 1.0: fundamental algorithms for scientific computing in Python. Nat. Methods 17, 261–272. https://doi.org/10.1038/s41592-019-0686-2.

Wilkening, M.H., 1952. Natural radioactivity as a tracer in the sorting of aerosols according to mobility. Rev. Sci. Instrum. 23, 13–16. https://doi.org/10.1063/1.1746056.

Zahorowski, W., Chambers, S.D., Henderson-Sellers, A., 2004. Ground based radon-222 observations and their application to atmospheric studies. Journal of Environmental Radioactivity. Elsevier, pp. 3–33. https://doi.org/10.1016/j.jenvrad.2004.03.033.